

1 Multiple Representation in Primate SI: A View from a Window on the Brain

A. W. Roe · R. M. Friedman · L. M. Chen


1	<i>Functional Representation in Primary Somatosensory Cortex (SI)</i>	2
1.1	Multiple Topographic Maps in SI	2
1.2	Hierarchical Relationship between Areas 3b and 1	2
1.3	Representation of Multiple Cutaneous Modalities in Areas 3b and 1	3
1.3.1	Psychophysical and Peripheral Channels	3
1.3.2	Anatomical and Physiological Pathways	4
1.3.3	Cortical Domains for Tactile Features	4
2	<i>Intrinsic Signal Optical Imaging in Primate SI</i>	5
2.1	The Methodology	5
2.1.1	Measuring Intrinsic Optical Signals	5
2.1.2	Signal Characteristics	5
2.1.3	Caveats in Interpretation	6
2.2	Optical Imaging of Cortical Somatotopy	6
2.2.1	Somatotopic Maps	6
2.2.2	New World Monkeys	7
2.3	Modality Domains in SI	8
2.3.1	Vibrotactile Activation	8
2.3.2	Vibrotactile Segregation	8
2.3.3	Vector Analysis	8
2.3.4	Neural Cortical Representation	9
2.4	Relationship of Vibrotactile Domains to Topography	10
2.5	Are There Pinwheels?	10
3	<i>Summary Model of SI Organization</i>	11

Abstract: This chapter summarizes recent findings regarding the functional organization of primary somatosensory cortex (SI) in primates when viewed through ‘windows’ on the brain with optical imaging methodologies. These views have confirmed previous knowledge regarding topographic organization in SI. They have also revealed the presence of functional domains for the processing of different sensory tactile modalities (pressure, flutter, and vibration domains). Surprisingly, the representation of these tactile modalities is quite distinct in organization from that of visual modalities (form, color, and depth) in visual cortex. Rather, tactile modality maps appear similar to visual orientation maps in primate visual cortex. Implications of these findings for the relationship of cortical organization to the sensory scene are discussed.

List of Abbreviations: SI, primary somatosensory cortex; SII, second somatosensory area; PV, parietal ventral area; SA, slowly adapting; RA, rapidly adapting; PC, pacinian; VPL, ventral posterior lateral; VPI, ventroposterior inferior; CCD, charge coupled device; V1, primary visual cortex; V2, second visual area; V4, fourth visual area; IT, inferotemporal cortex

1 Functional Representation in Primary Somatosensory Cortex (SI)

1.1 Multiple Topographic Maps in SI

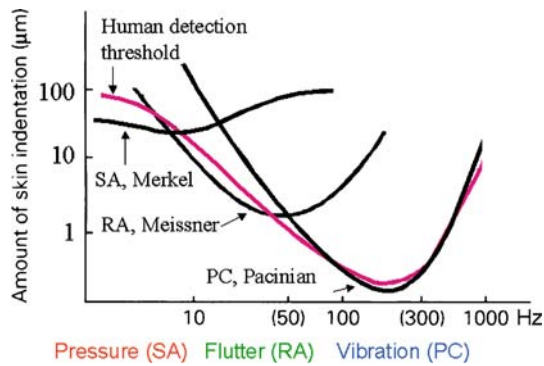
Primate primary somatosensory cortex (SI) in the postcentral gyrus contains four complete topographic maps of the body surface that fall within the architectonically defined Brodmann’s Areas 3a, 3b, 1, and 2 (e.g., Woolsey et al., 1942; Powell and Mountcastle, 1959; Kaas et al., 1979; Nelson et al., 1980; Sur et al., 1982; Pons et al., 1985, 1987)  *Figure 1-1*. Areas 3b and 1 receive input primarily from cutaneous afferents where areas 3a and 2 receive input from deep afferents (muscle spindles and joints) (e.g., Tanji and Wise, 1981). Other parietal areas, such as Areas 5 and 7, also process somatosensory information (Murray and Mishkin, 1984; Dong et al., 1994; Burton et al., 1997; Duhamel et al., 1998; Debowy et al., 2001). Somatotopic maps are also found laterally in second somatosensory area (SII) and the adjacent parietal ventral area (PV) (Burton and Fabri, 1995; Krubitzer et al., 1995) and there are other somatosensory areas in insular cortex that receive cutaneous and visceral information (Robinson and Burton, 1980; Schneider et al., 1993; Craig, 2003).

1.2 Hierarchical Relationship between Areas 3b and 1

Numerous studies suggest a hierarchical relationship between Area 3b and Area 1. Ablations of Area 3a and 3b leave Area 1 unresponsive, consistent with anatomy studies that show that Area 1 receives the bulk of its input from Area 3b. These findings suggest that direct thalamic inputs to Area 1 play either a weak or a modulatory role in cutaneous information processing (Garraghty et al., 1990). In comparison with cells of Area 1, response properties of cells in Area 3b can be described as relatively simple or closer to the physical aspects of the stimulus. Area 3b neurons (and layer 4 neurons in Area 1) have receptive fields confined to single-digit tips; in contrast, Area 1 neurons recorded in supra- or infragranular layers integrate over larger areas of skin, often spanning multiple-digit tips (Mountcastle and Powell, 1959; Hyvarinen and Poranen, 1978; Costanzo and Gardner, 1980; Iwamura et al., 1983; Sur et al., 1980, 1985). In concert with a greater degree of integration in Area 1, intrinsic connections within Area 1 are more extensive than those in Area 3b (Burton and Fabri, 1995). Both SA (slowly adapting) and RA (rapidly adapting) responsive cells are commonly found in Area 3b, whereas Area 1 is characterized by a predominance of RA cells and cells responsive to motion and orientation (Warren et al., 1986; Nelson et al., 1991). Although both mechanoreceptors and RA cells are responsive to textured surfaces, the firing patterns of slowly-adapting type I mechanoreceptors cells are more closely tied with roughness and texture features (Connor and Johnson, 1992; Blake et al., 1997). These findings could suggest a stronger role of Area 3b in fine spatial pattern

Figure 1-2

Psychophysically determined thresholds for detection of different frequencies of vibrotactile stimulation. Peak thresholds are around 1Hz, 30Hz, and 200Hz



respectively) (Torebjork and Ochoa, 1980; Vallbo, 1981). Psychophysics studies fail to find vibrotactile masking and adaptation between stimulus frequencies that produce pressure (0.5Hz), flutter (20Hz), and vibratory sensations (200Hz) (Gescheider et al., 1979, 1985; Bolanowski et al., 1988). In addition, frequency-specific electrical stimulation of a cortical RA-dominated site in Area 3b mimics the effect of stimulating RA receptors of the skin (Romo et al., 1998). Remarkably, even the transfer of tactile learning from one digit to another is modality-specific (Harris et al., 2001). These studies suggest a marked degree of separation in the experiences of pressure, flutter, and vibration, mediated by separate populations of receptors that remain separate in their central projections, and perhaps even to higher cortical areas involved in tactile learning and memory (see also Romo et al., 2000). Thus, both psychophysics and neurophysiology studies suggest some degree of modality-specific functional segregation in somatosensory cortex.

1.3.2 Anatomical and Physiological Pathways

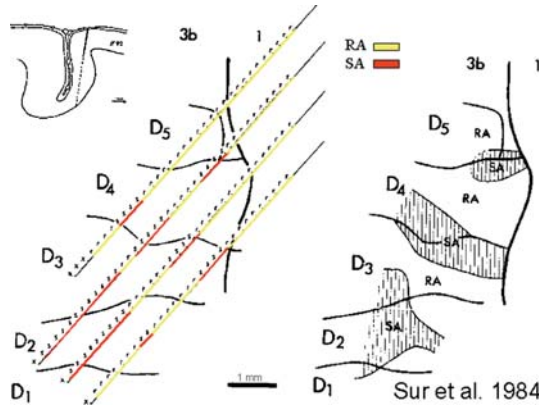
Anatomical and physiological evidence also suggest parallel modality-specific pathways, from periphery through the dorsal column nuclei, to the thalamus, and into early somatosensory cortical areas. Dykes et al. (1981) have described the segregation of RA, SA, and PC responses in the VPL and VPI. Jones and colleagues (1982) have suggested that “rods” of topography and modality-specific cells project to similar modality-specific bands in Area 3b, and perhaps Area 1. Connections between Areas 3b and 1 are topographically homotopic, with feedforward projections being more robust than feedback (e.g., Jones and Powell, 1969; Jones et al., 1978; Cusick et al., 1985; Burton and Fabri, 1995). Using 2-deoxyglucose labeling methods combined with anatomical tracer injections, Juliano et al. (1990) suggested that excitatory information is transmitted from Area 3b to Area 1 in a way that connects clusters of cells with similar response properties.

1.3.3 Cortical Domains for Tactile Features

However, there is limited evidence to show whether different tactile features form multiple functional domains within each of Areas 3a, 3b, 1, and 2. Perhaps the best evidence for functional domains within SI comes from electrophysiological mapping studies describing zones of neurons with SA, RA, and PC mechanoreceptor responses within Area 3b (Paul et al., 1972; Sur et al., 1981, 1984; Sretavan and Dykes, 1983). [Figure 1-3](#) Based on densely spaced electrode penetrations, Sur et al. (1981, 1984) found a segregation of SA and RA cells in the middle layers of Area 3b and suggested that these are organized in

■ Figure 1-3

Electrophysiological evidence of modality-specific segregation in Area 3b (from Sur et al., 1984). Based on this and other studies, it was hypothesized that Area 3b contains alternating bands or zones of pressure and flutter domains



irregular antero-posterior “bands.” This groundbreaking work was the first to suggest the presence of multiple maps in single cortical areas in SI. However, the limitations of electrophysiological mapping still leave open many questions regarding the degree of modality-specific segregation in Area 3b and its architecture. It is not clear whether SA/RA segregation in the middle layers implies some segregation in the superficial or deep layers of cortex. Whether a third map for PC responses exists is also unknown. It is also unknown whether Area 1, which is tightly associated with Area 3b, contains any functional organization for vibrotactile modality.

2 Intrinsic Signal Optical Imaging in Primate SI

2.1 The Methodology

2.1.1 Measuring Intrinsic Optical Signals

Optical imaging of intrinsic cortical signals is a method based on the activity-dependent reflectance changes of cortical tissue. The imaging procedure uses a charge-coupled device (CCD) camera to record the minute changes in optical absorption that accompanies cortical activity (Blasdel and Salama, 1986; Grinvald et al., 1986; Ts'o et al., 1990; Bonhoeffer and Grinvald, 1996). By presenting appropriate stimuli during optical imaging, the functional organizations of the sensory cortices can be mapped at high resolution. Although spiking response of single neurons is often predictive of the preference of the imaged domain (e.g., Bonhoeffer and Grinvald, 1991), it is known that both spiking and subthreshold sources contribute to the intrinsic optical signal.

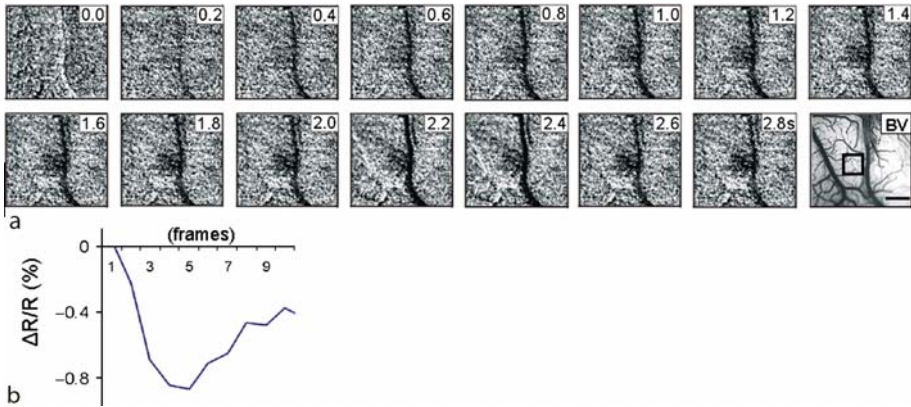
2.1.2 Signal Characteristics

The magnitude (typically in the 0.1–1.0% range) and timecourse of reflectance change is dependent on the illumination wavelength used (Bonhoeffer and Grinvald, 1996). In visual cortex, the typical

time course under 600–630nm illuminant and 2–3s stimulation peaks in 2–3s, followed by an undershoot that recovers in 4–5s. The optical signal is similar in SI (Figure 1-4; Chen et al., 2001; Friedman et al., 2004). Longer illumination wavelengths and longer stimulation periods produce longer signal timecourses (cf. Tommerdahl et al., 1999).

Figure 1-4

Timecourse of optical signal. (a) A series of images showing the temporal development of intrinsic cortical response (indentation of D2, pentothal anesthesia). Each frame 200ms. BV, blood vessel map. Scale bar: 1mm. (b) Magnitude of reflectance change (in box at BV)



2.1.3 Caveats in Interpretation

The relationship of the intrinsic signal to neural activity is by nature indirect and must be interpreted carefully. In visual cortex, due to the clustered nature of visual functional organization and microvascular relationships, the correlation of this signal with local neural excitatory response is strongly supported (e.g., Grinvald et al., 1986; Bonhoeffer et al., 1995; Roe and Ts'o, 1995, 1999; Rao et al., 1997; Issa et al., 2000). In somatosensory and auditory cortices, neurophysiological/imaging correlations also exist (cf. Bakin et al., 1996; Harel et al., 2000; Chen et al., 2001; Spitzer et al., 2001). Interpretation of optical images requires careful attention to stimulus design, multiple types of image analysis, and, if possible, accompanying electrophysiological recordings. For example, the presence of strong optical signal can indicate either a strong uniform stimulus-specific response or a diversity of response dominated by one particular component. In differential images, lack of response may be indistinguishable from equal responsiveness to opposing stimuli. Finally, it is important to bear in mind that the apparent organization of a cortical area as revealed by optical imaging is a direct function of the stimulus used to probe its organization.

2.2 Optical Imaging of Cortical Somatotopy

2.2.1 Somatotopic Maps

Optical imaging has been used in the study of somatosensory representation in rats (Masino and Frostig, 1993, 1996; Goldreich et al., 1998; Sheth et al., 1998), nonhuman primates, and humans (Cannestra et al., 1998; Schwartz et al., 2004). In the nonhuman primate, studies of somatotopy have produced images of the body map in the squirrel monkey (radial interdigital pad, D2 fingertip, and similar sites on the leg and foot)

(Tommerdahl et al., 1999), distal fingerpads of the squirrel monkey (Chen et al., 2001; Tommerdahl et al., 2002), and Area 1 of the Macaque monkey (Shoham and Grinvald, 2001). These have, in general, been consistent with the previously described somatotopic maps (e.g., Sur et al., 1982).

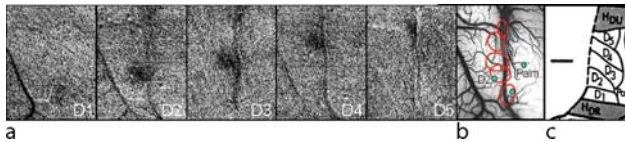
2.2.2 New World Monkeys

New World monkeys are an attractive species for optical imaging studies because their lissencephalic cortex allows unobstructed viewing of multiple visual cortical areas (cf. for visual cortex Malach et al., 1994; Xu et al., 2004; Roe et al., 2005). Furthermore, New World monkeys have been studied extensively in physiological, anatomical, and behavioral studies, making them prime candidates for studies of functional organization of sensation and sensory behavior. In the squirrel monkey, we have observed an orderly topographical map of the fingerpads within Area 3b (▶ [Figure 1-5](#)), consistent with the progression of maps determined with electrophysiological mapping (e.g., Sur et al., 1982; Merzenich et al., 1987). Activation sites were focal, measuring 0.5–1 mm in size.

In New World monkeys, it is also possible to simultaneously image multiple cortical areas, including Areas 3a, 3b, 1, and 2. As shown in ▶ [Figure 1-6](#), the functional organization of SI in New World monkeys largely parallels those in Old World monkeys (cf. Sur et al., 1982). Stimulation of a single digit produces activation in Areas 3b and 1 in a topographically predictable manner (cf. Chen et al., 2002, 2005).

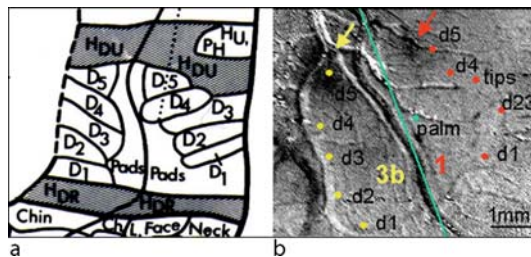
■ Figure 1-5

Optical images of digit tip topography in Area 3b in squirrel monkey. (a) Five images obtained in response to indentation of digits D1 (thumb) to D5, respectively. Dark pixels indicate cortical activation (decrease in cortical reflectance). (b) Locations of D1–D5 activation zones are indicated by red circles overlaid on the blood vessel map. Green dots are locations of electrical recordings. (c) Topography consistent with published maps of digit topography (a, b from Chen et al., 2001; c from Sur et al., 1982)



■ Figure 1-6

Optical imaging of multiple cortical areas in SI of squirrel monkey. (a) Digit topography in Areas 3b and 1 (Sur et al., 1982). (b) Optical image of Area 3b and Area 1 to indentation of digit D5. Electrophysiological mapping of 3b (yellow dots) and 1 (red dots). Note that D5 activation zones (dark zones indicated by arrows) correlate well with electrophysiological map



2.3 Modality Domains in SI

2.3.1 Vibrotactile Activation

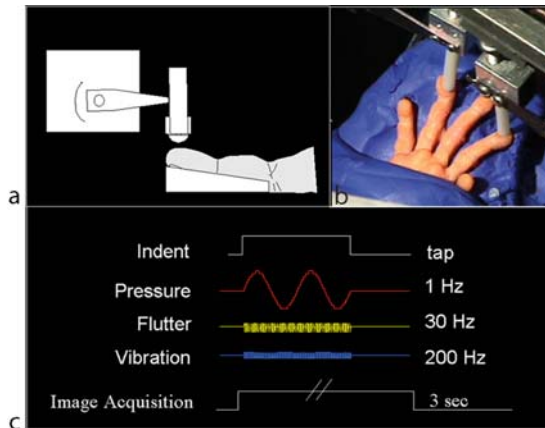
As reported by Tommerdahl et al. (1996, 1998), mapping of modality-specific responses revealed vibrotactile response in Areas 3b and 1, and preferential response to skin heating in Area 3a. Comparison of flutter and vibration response revealed that extended vibration stimuli induced an initial increase in signal followed by a broad decrease, reminiscent of inhibitory influences described in neurophysiology studies (Tommerdahl et al., 1999).

2.3.2 Vibrotactile Segregation

Segregation of RA, SA, and PC responsiveness in Area 3b (Chen et al., 2001) and Area 1 (Friedman et al., 2004) of the squirrel monkey has been reported. Vibrotactile stimulation of the digit fingerpads at frequencies that produce the sensations of pressure (1Hz), flutter (30Hz), and vibration (200Hz) were used in the anesthetized squirrel monkey (▶ [Figure 1-7](#)). These stimuli produced characteristic SA-dominated, RA-dominated, or PC-dominated responses, respectively. In some penetrations, single vibrotactile modalities were predominant; however, in other penetrations, mixed responses were obtained.

■ Figure 1-7

Stimulation of digit tips. (a) Vibrotactile stimuli applied by a 3-mm diameter probe driven by a force feedback controlled motor. (b) Digits are secured by pegs glued to fingernails and inserted into plasticine. Two digit tips are stimulated with two probes controlled by two separate motors. (c) Temporal timecourse of each of three vibrotactile stimuli that induce pressure (1Hz), flutter (30Hz), and vibration (200Hz). Images acquisition (3s) of cortical response during each vibrotactile stimulus



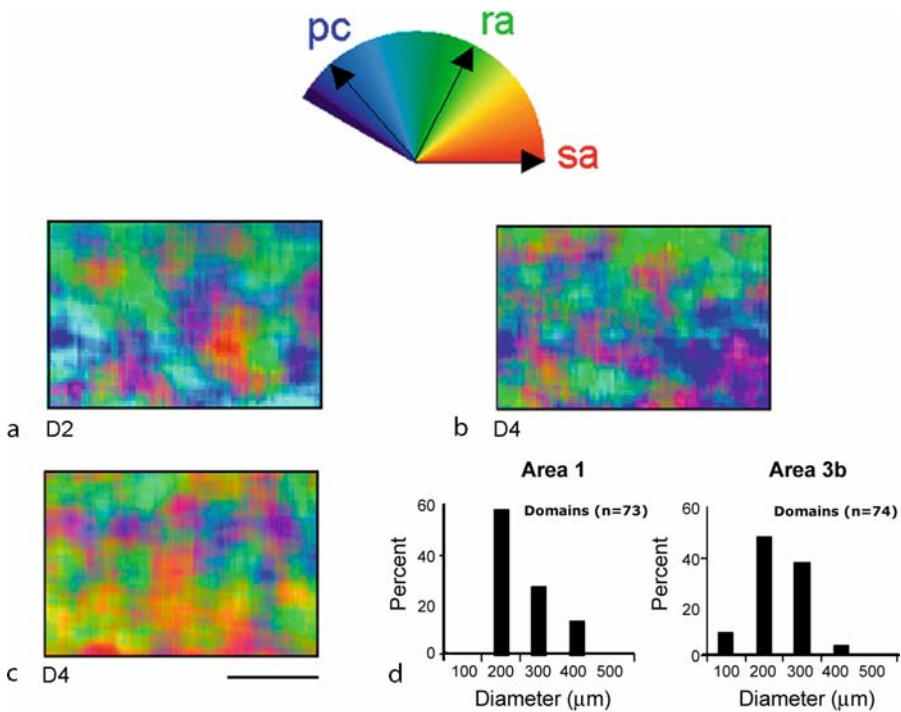
2.3.3 Vector Analysis

Intrinsic signal optical maps were obtained in response to each of these stimuli. A vector summation method was used to determine a pixel-by-pixel weighted response to the pressure, flutter, and vibration stimuli (similar to that used for visual cortical orientation maps, methodology details are described in Friedman et al., 2004). Clusters of pixels with saturated color would be evident only if one vector magnitude dominated the other two. Three examples of such pixel-wise SA/RA/PC vector summation are illustrated in

Figure 1-8a–c. Pixel locations with a dominant SA response appear bright red, those with a dominant RA response appear bright green, and those with a dominant PC response appear bright blue. Patches of cortex that are coded white indicate areas exhibiting strong response to each of the pressure, flutter, and vibratory stimuli. In each map, we observed an irregular, interdigitating pattern of pressure (red), flutter (green), and vibration (blue) domains interspersed, in some maps, with domains of mixed preference (e.g., light blue). These domains were typically 200–300 μm in size in both Area 3b and Area 1 (Figure 1-8d).

Figure 1-8

Modality maps in SI. *Top*: Vibrotactile frequency-specific responses are plotted in different directions of color space (red: SA, 1Hz; green: RA, 30Hz; blue: PC, 200Hz). a–c; Three cases: vector maps obtained through pixel-by-pixel vector summation. Domains dominated by single colors indicate regions preferentially responsive to a single vibrotactile frequency. Scale bar: 1 mm. (d) Size distribution of vibrotactile domains in Area 1 (*left*) and Area 3b (*right*)



2.3.4 Neural Cortical Representation

Prior electrophysiology studies have not observed modular domains for vibrotactile stimuli in Area 1 (Costanzo and Gardner, 1980, Iwamura et al., 1993). A possible reason is that the small patch size of the modular domains in Area 1 revealed in our optical images would be difficult to discern solely with single and multiunit electrophysiology. In addition, previous studies focused on the adaptation (rapidly or slowly adapting) properties of neurons in Area 1 rather than on whether the neurons were integrating the information originating from SA, RA, or PC mechanoreceptors. When we examined these maps

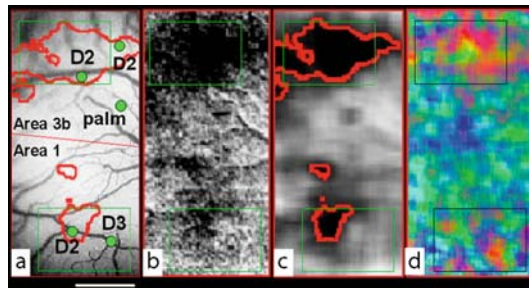
electrophysiologically, we found that, consistent with previous studies (Sur et al., 1984; Iwamura et al., 1993), single electrophysiological penetrations contained a mixture of neurons with SA, RA, and/or PC responses and single neurons that contained mixed responses. Often, we recorded neurons with solely rapidly adapting responses or mixed slowly and rapidly adapting responses. Thus, our data suggest that individual domains in Areas 3b and 1 contain neurons with a range of response properties, but coding of function within each domain is dominated by one modality.

2.4 Relationship of Vibrotactile Domains to Topography

It is evident that the modality-specific response extends beyond the classically defined topographic map as revealed by simple indentation stimuli. As shown in [Figure 1-9b](#), an indentation stimulus (which activates all three receptor types) to digit D2 produces a fairly focal activation in both Area 3b and Area 1 (outline in red in [Figure 1-9c](#)). In response to pressure, flutter, and vibration stimulation, the vector summation map reveals that the strongest responses (most saturated red, green, and blue regions)

Figure 1-9

Relationship of topography and vibrotactile response. D2 activation in Areas 3b and 1. (a) Vessel map. D2 activations in Area 3b (above) and Area 1 (below). (b,c) Raw and filtered image of D2 indentation. Red outline delineates strongest activation zones. (d) Modality vector map (red, green, blue: response for SA, RA, and PC, respectively) shows strongest activation in centers of D2 activation and weaker activation outside of D2 zones. Scale bar: 1 mm. (Friedman et al., 2004)



correspond with the topographic digit locations. However, clustered responses, though weaker, are also evident away from the location of D2 representation (outside the boxes). This additional nontopographic activation is reminiscent of the finding in visual cortex, in which complete orientation maps are obtained even though only a single eye is stimulated (Blasdel, 1992). Thus, modality maps and topographic maps exhibit some degree of independence. Whether this extended nontopographic region of activation is due to spiking and/or subthreshold activity remains to be determined.

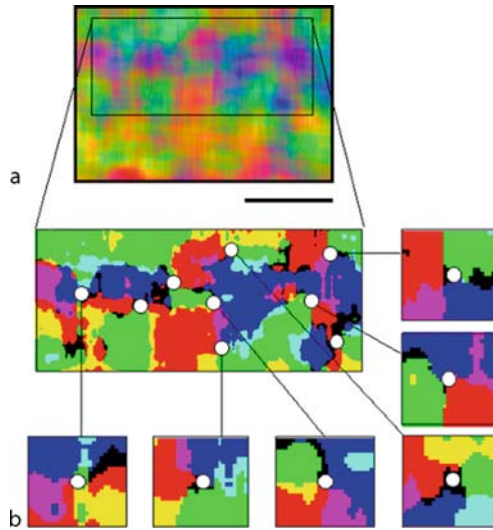
2.5 Are There Pinwheels?

In optical imaging studies of visual cortex, orientation pinwheels have received a great deal of attention. Pinwheels are locations (singularities) in orientation maps around which the orientation preference changes smoothly. Although the locations, density, stability, and function of pinwheels in optical maps has been a topic of much controversy (e.g., Bonhoeffer and Grinvald, 1991; Bartfeld and Grinvald, 1992; Obermayer et al., 1997; Swindale, 2000; Schummers et al., 2002; Polimeni et al., 2005), they have become a cornerstone of cortical functional architecture. The key feature of pinwheels is that they are points around which a parameter (such as contour orientation) varies continuously. Although further studies are needed,

the possibility that vibrotactile maps in SI contain pinwheel-like features has been suggested (Friedman et al., 2004). In contrast to some visual cortical maps that demonstrate clear discontinuities, response preferences in SI vibrotactile maps appear to vary continuously, giving rise to an appearance more reminiscent of visual orientation maps. As shown in [▶ Figure 1-10](#), possible singularity sites are

■ **Figure 1-10**

Possible pinwheel centers in SI. (a) Same map shown in [▶ Figure 1-9c](#). (b) Expanded and thresholded portion of (a) Possible pinwheels marked by white dots, shown expanded in nearby panels. Note clockwise and counter-clockwise SA (red), RA (green), PC (blue) rotations



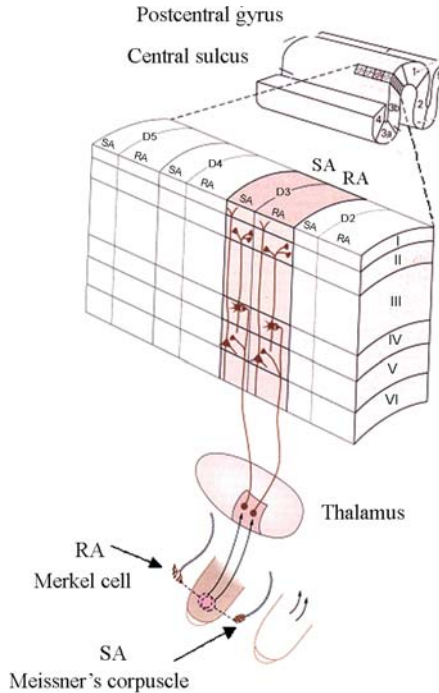
those around which a rotation of vibrotactile frequency can be observed. Whether these rotations are continuous changes in frequency or simply convergence points of discrete frequency clusters remains to be investigated.

3 Summary Model of SI Organization

The finding that somatosensory cortical domains are roughly 200–300 μm in size strengthens the view that modularity is a common organizational feature of cortical representation. Cortical domains of similar size have been described in multiple cortical areas [in V1 and V2 (see Roe, 2003 for review), and V4 (Felleman et al., 1997), IT (Tsunoda et al., 2001), Area 7 (Siegel et al., 2003), and in prefrontal areas (Kritzer and Goldman-Rakic, 1995)]. These findings suggest a revision of previous views of SI organization, which were based primarily on electrophysiological recordings. Previously, each cortical “hypercolumn” was thought to contain segregated Sa and Ra columns innervated predominantly by thalamocortical fibers of a single vibrotactile modality ([▶ Figure 1-11](#), Sur et al., 1980). Optical imaging evidence now suggests a modification of this view ([▶ Figure 1-12](#)). As shown by reconstruction of single thalamocortical arbors (Garrahy et al., 1989), inputs to SI have multiple arbors (200–300 μm in size) that span several millimeters of cortex (see also Jones et al., 1982). These and other corticocortical arbors are likely to give rise to clustered activations that have been observed in 2-deoxyglucose studies (Juliano 1981, 1990; Juliano and Whistel, 1987; cf. Burton and Fabri, 1995). Such arbors could give rise either to an array of discrete clusters or, by

■ **Figure 1-11**

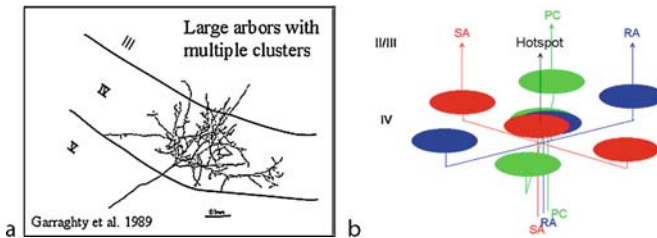
Traditional view of SI organization. (from Kandel & Schwartz)



varying arbor overlap, continuous modality maps. Thus, regions dominated by single SA, RA, or PC inputs would give rise to SA (red), RA (green), or PC (blue) domains. Regions of some overlap would appear as magenta or yellow-green colors (not depicted). In addition, regions of high SA, RA, and PC overlap could

■ **Figure 1-12**

Proposed model of vibrotactile representation in SI. (a) Thalamocortical arbors in SI have multiple clusters extending across millimeters of cortex (Garraghty et al., 1989). (b) Single SA, RA, or PC fibers terminate in layer IV with three arbors (colored disks). These arbors project in turn to superficial layers II/III. Thus, some cortical columns are dominated by a single SA, RA, or PC input, whereas others have mixed input (overlapping disks)



underlay the so-called hotspots commonly described in SI receptive fields (in optical images, these locations would appear as black, gray, or white domains); these would be well activated by broadband stimuli such as skin indentation. Other arbors extend to nontopographic locations away from the hotspot and locally

establish some degree of modality-specific dominance (cf. [Figure 1-10](#)). Thus, not unlike the way horizontal iso-orientation networks in V1 give rise to resulting orientation map structure, the observed maps result from overlapping horizontal networks of patchy, modality-specific dominance. In sum, in the revised view, each digit representation is served by collections of interdigitating SA, RA, and PC columns. The effect of topographic stimulation is therefore no longer so discrete and can, under certain stimulation conditions, have nontopographic consequences.

References

- Bakin JS, Kwon MC, Masino SA, Weinberger NM, Frostig RD. 1996. Suprathreshold auditory cortex activation visualized by intrinsic signal optical imaging. *Cereb Cortex* 6: 120-130.
- Bartfield E, Grinvald A. 1992. Relationships between orientation-preference pinwheels, cytochrome oxidase blobs, and ocular-dominance columns in primate striate cortex. *Proc Natl Acad Sci USA* 89(24): 11905-11909.
- Blake DT, Hsiao SS, Johnson KO. 1997. Neural coding mechanisms in tactile pattern recognition: The relative contributions of slowly and rapidly adapting mechanoreceptors to perceived roughness. *J Neurosci* 17: 7480-7489.
- Blasdel GG, Salama G. 1986. Voltage-sensitive dyes reveal a modular organization in monkey striate cortex. *Nature* 321: 579-585.
- Blasdel GG. 1992. Differential imaging of ocular dominance and orientation selectivity in monkey striate cortex. *J Neurosci* 12: 3115-3138.
- Bolanowski SJ Jr, Gescheider GA, Verrillo RT, Checkosky CM. 1988. Four channels mediate the mechanical aspects of touch. *J Acoust Soc Am* 84: 1680-1694.
- Bonhoeffer T, Grinvald A. 1991. Iso-orientation domains in cat visual cortex are arranged in pinwheel-like patterns. *Nature* 353: 429-431.
- Bonhoeffer T, Kim DS, Malonek D, Shoham D, Grinvald A. 1995. Optical imaging of the layout of functional domains in Area 17 and across the Area 17/18 border in cat visual cortex. *Eur J Neurosci* 7: 1973-1988.
- Bonhoeffer T, Grinvald A. 1996. Brain mapping: The methods. Toga AW, Mazziotta JC, editors. New York: Academic Press; pp. 55-97.
- Burton H, Fabri M. 1995. Ipsilateral intracortical connections of physiologically defined cutaneous representations in areas 3b and 1 of macaque monkeys: Projections in the vicinity of the central sulcus. *J Comp Neurol* 355: 508-538.
- Burton H, Sinclair RJ, Hong SY, Pruetz JR Jr, Whang KC. 1997. Tactile-spatial and cross-modal attention effects in the second somatosensory and 7b cortical areas of rhesus monkeys. *Somatosens Mot Res* 14(4): 237-267.
- Cannestra AF, Black KL, Martin NA, Cloughesy T, Burton JS, et al. 1998. Topographical and temporal specificity of human intraoperative optical intrinsic signals. *Neuroreport* 9: 2557-2563.
- Carlson M. 1981. Characteristics of sensory deficits following lesions of Brodmann's areas 1 and 2 in the postcentral gyrus of *Macaca mulatta*. *Brain Res* 204(2): 424-430.
- Carlson M. 1984. Development of tactile discrimination capacity in *Macaca mulatta*. II. Effects of partial removal of primary somatic sensory cortex (Sml) in infants and juveniles. *Brain Res* 318: 83-101.
- Chen LM, Friedman RM, Ramsden BM, La Motte RH, Roe AW. 2001. Fine-scale organization of primary somatosensory cortex (Area 3b) in the squirrel monkey revealed with intrinsic optical imaging. *J Neurophysiol* 86: 3011-3029.
- Chen LM, Heider B, Healy FL, Ramsden BR, Williams GV, et al. 2002. A chamber and artificial dura method for long-term optical imaging in primates. *J Neurosci* 113: 41-49.
- Chen LM, Friedman RM, Roe AW. 2005. Optical imaging of SI topography in anesthetized and awake squirrel monkeys. *J Neurosci* 25(33): 7648-7659.
- Cohen RH, Vierck CJ. 1993. Population estimates for responses of cutaneous mechanoreceptors to a vertically indenting probe on the glabrous skin of monkeys. *Exp Brain Res* 94: 105-119.
- Connor CE, Johnson KO. 1992. Neural coding of tactile texture: Comparison of spatial and temporal mechanisms for roughness perception. *J Neurosci* 12: 3414-3426.
- Costanzo RM, Gardner EP. 1980. A quantitative analysis of responses of direction sensitive neurons in somatosensory cortex of awake monkeys. *J Neurophysiol* 43: 139-1341.
- Craig AD. 2003. Pain mechanisms: labeled lines versus convergence in central processing. *Annu Rev Neurosci* 26: 1-30.
- Cusick CG, Steindler DA, Kaas JH. 1985. Corticocortical and collateral thalamocortical connections of postcentral somatosensory cortical areas in squirrel monkeys: A double-labeling study with radiolabeled wheatgerm agglutinin and wheatgerm agglutinin conjugated to horseradish peroxidase. *Somatosens Res* 3: 1-31.
- Debowy DJ, Ghosh S, Ro JY, Gardner EP. 2001. Comparison of neuronal firing rates in somatosensory and posterior parietal cortex during prehension. *Exp Brain Res* 137(3-4): 269-291.

- Dong WK, Chudler EH, Sugiyama K, Roberts VJ, Hayashi T. 1994. Somatosensory, multisensory, and task-related neurons in cortical area 7b (PF) of unanesthetized monkeys. *J Neurophysiol* 72(2): 542-564.
- Duhamel JR, Colby CL, Goldberg ME. 1998. Ventral intraparietal area of the macaque: Congruent visual and somatic response properties. *J Neurophysiol* 79(1): 126-136.
- Dykes RW, Sur M, Merzenich MM, Kaas JH, Nelson RJ. 1981. Regional segregation of neurons responding to quickly adapting, slowly adapting, deep and pacinian receptors within thalamic ventroposterior lateral and ventroposterior inferior nuclei in the squirrel monkey (*Saimiri sciureus*). *Neurosci* 6: 1687-1692.
- Felleman DJ, Xiao Y, McClendon E. 1997. Modular organization of occipito-temporal pathways: Cortical connections between visual area 4 and visual area 2 and posterior inferotemporal ventral area in macaque monkeys. *J Neurosci* 17(9): 3185-3200.
- Friedman RM, Chen LM, Roe AW. 2004. Modality maps within primate somatosensory cortex. *Proc Natl Acad Sci USA* 101: 12724-12729.
- Garraghty PE, Pons TP, Sur M, Kaas JH. 1989. The arbors of axons terminating in middle cortical layers of somatosensory area 3b in owl monkeys. *Somatosens Mot Res* 6(4): 401-411.
- Garraghty PE, Florence SL, Kaas J. 1990. Ablations of areas 3a and 3b of monkey somatosensory cortex abolish cutaneous responsiveness in area 1. *Brain Res* 528: 165-169.
- Gescheider GA, Frisina RD, Verrillo RT. 1979. Selective adaptation of vibrotactile thresholds. *Sens Processes* 3: 37-48.
- Gescheider GA, Sklar BF, Van Doren CL, Verrillo RT. 1985. Vibrotactile forward masking: Psychophysical evidence for a triplex theory of cutaneous mechanoreception. *J Acoust Soc Am* 78(2): 534-543.
- Goldreich D, Peterson BE, Merzenich MM. 1998. Optical imaging and electrophysiology of rat barrel cortex. II. Responses to paired-vibrissa deflections. *Cereb Cortex* 8: 184-192.
- Grinvald A, Lieke E, Frostig RD, Gilbert CD, Wiesel TN. 1986. Functional architecture of cortex revealed by optical imaging of intrinsic signals. *Nature* 324: 361-364.
- Harel N, Mori N, Sawada S, Mount RJ, Harrison RV. 2000. Three distinct auditory areas of cortex (AI, AII, and AAF) defined by optical imaging of intrinsic signals. *Neuroimage* 11: 302-312.
- Harris JA, Harris IM, Diamond ME. 2001. The topography of tactile learning in humans. *J Neurosci* 21: 1056-1061.
- Hyvarinen J, Poranen A. 1978. Movement-sensitive and direction and orientation-selective cutaneous receptive fields in the hand area of the post-central gyrus in monkeys. *J Physiol* 283: 523-537.
- Issa NP, Trepel C, Stryker MP. 2000. Spatial frequency maps in cat visual cortex. *J Neurosci* 20: 8504-8514.
- Iwamura Y, Tanaka M, Sakamoto M, Hikosaka O. 1983. Converging patterns of finger representation and complex response properties of neurons in Area 1 of the first somatosensory cortex of the conscious monkey. *Exp Brain Res* 51: 327-337.
- Johansson RS, Landstrom U, Lundstrom R. 1982. Responses of mechanoreceptive afferent units in the glabrous skin of the human hand to sinusoidal skin displacements. *Brain Res* 244: 17-25.
- Jones EG, Powell TPS. 1969. Connexions of the somatic sensory cortex of the rhesus monkey. I. Ipsilateral connections. *Brain* 92: 477-502.
- Jones EG, Coulter JD, Hendry SHC. 1978. Intracortical connectivity of architectonic fields in the somatic sensory, motor and parietal cortex of monkeys. *J Comp Neurol* 181: 291-347.
- Jones EG, Friedman DP, Hendry SHC. 1982. Thalamic basis of place- and modality-specific columns in monkey somatosensory cortex: A correlative anatomical and physiological study. *J Neurophysiol* 48: 545-568.
- Juliano SL, Whitsel BL. 1987. A combined 2-deoxyglucose and neurophysiological study of primate somatosensory cortex. *J Comp Neurol* 263: 514-525.
- Juliano SL, Hand PF, Whitsel BL. 1981. Patterns of increased metabolic activity in somatosensory cortex of monkeys *Macaca fascicularis*, subjected to controlled cutaneous stimulation: A 2-deoxyglucose study. *J Neurophysiol* 46: 1260-1284.
- Juliano SL, Friedman DP, Eskin DE. 1990. Corticocortical connections predict patches of stimulus-evoked metabolic activity in monkey somatosensory cortex. *J Comp Neurol* 298: 23-39.
- Kaas JH, Nelson RJ, Sur M, Lin CS, Merzenich MM. 1979. Multiple representations of the body within the primary somatosensory cortex of primates. *Science* 204: 521-523.
- Kritzer MF, Goldman-Rakic PS. 1995. Intrinsic circuit organization of the major layers and sublayers of the dorsolateral prefrontal cortex in the rhesus monkey. *J Comp Neurol* 359: 131-143.
- Krubitzer L, Clarey J, Tweedale R, Elston G, Calford M. 1995. A redefinition of somatosensory areas in the lateral sulcus of macaque monkeys. *J Neurosci* 15: 3821-3839.
- La Motte RH, Mountcastle VB. 1975. Capacities of humans and monkeys to discriminate vibratory stimuli of different frequency and amplitude: A correlation between neural events and psychological measurements. *J Neurophysiol* 38: 539-559.
- Malach R, Tootell RBH, Malonek D. 1994. Relationship between orientation domains, cytochrome oxidase stripes, and intrinsic horizontal connections in squirrel monkey area V2. *Cereb Cortex* 4: 151-165.

- Masino SA, Kwon MC, Dory Y, Frostig RD. 1993. Characterization of functional organization within rat barrel cortex using intrinsic signal optical imaging through a thinned skull. *Proc Natl Acad Sci USA* 1993 Nov 1; 90(21): 9998-10002.
- Masino SA, Frostig RD. 1996. Quantitative long-term imaging of the functional representation of a whisker in rat barrel cortex. *Proc Natl Acad Sci USA* 93: 4942-4947.
- Merzenich MM, Nelson RJ, Kaas JH, Stryker MP, Jenkins WM, et al. 1987. Variability in hand surface representations in areas 3b and 1 in adult owl and squirrel monkeys. *J Comp Neurol* 258: 281-296.
- Mountcastle VB, Powell TPS. 1959. Neural mechanisms subserving cutaneous sensibility, with special reference to the role of afferent inhibition in sensory perception and discrimination. *Bull Johns Hopkins Hosp* 105: 201-232.
- Mountcastle VB, La Motte RH, Carli G. 1972. Detection thresholds for stimuli in humans and monkeys: Comparison with threshold events in mechanoreceptive afferent nerve fibers innervating the monkey hand. *J Neurophysiol* 35: 122-136.
- Murray EA, Mishkin M. 1984. Relative contributions of SII and area 5 to tactile discrimination in monkeys. *Behav Brain Res* 11: 67-83.
- Nelson RJ, Sur M, Felleman DJ, Kaas JH. 1980. Representations of the body surface in postcentral parietal cortex of *Macaca fascicularis*. *J Comp Neurol* 192(4): 611-643.
- Nelson RJ, Smith BN, Douglas VD. 1991. Relationships between sensory responsiveness and premovement activity of quickly adapting neurons in areas 3b and 1 of monkey primary somatosensory cortex. *Exp Brain Res* 84: 75-90.
- Obermayer K, Blasdel GG. 1997. Singularities in primate orientation maps. *Neural Comput* 9: 555-575.
- Paul RL, Merzenich M, Goodman H. 1972. Representation of slowly and rapidly adapting cutaneous mechanoreceptors of the hand in Brodmann's areas 3 and 1 of *Macaca mulatta*. *Brain Res* 36: 229-249.
- Polimeni JR, Granquist-Fraser D, Wood RJ, Schwartz EL. 2005. Physical limits to spatial resolution of optical recording: clarifying the spatial structure of cortical hypercolumns. *Proc Natl Acad Sci USA* 102(11): 4158-4163.
- Pons TP, Garraghty PE, Cusick CG, Kaas JH. 1985. A sequential representation of the occiput, arm, forearm and hand across the rostrocaudal dimension of areas 1, 2 and 5 in macaque monkeys. *Brain Res* 335(2): 350-353.
- Pons TP, Wall JT, Garraghty PE, Cusick CG, Kaas JH. 1987. Consistent features of the representation of the hand in area 3b of macaque monkeys. *Somatosens Res* 4: 309-331.
- Powell TP, Mountcastle VB. 1959. The cytoarchitecture of the postcentral gyrus of the monkey *Macaca mulatta*. *Bull Johns Hopkins Hosp* 105: 108-131.
- Rao SC, Toth LJ, Sur M. 1997. Optically imaged maps of orientation preference in primary visual cortex of cats and ferrets. *J Comp Neurol* 87: 358-370.
- Robinson CJ, Burton H. 1980. Organization of somatosensory receptive fields in cortical areas 7b, retrosulcus, postauditory and granular insula of *M. fascicularis*. *J Comp Neurol* 192(1): 69-92.
- Robinson CJ, Burton H. 1980b. Somatic submodality distribution within the second somatosensory (SII), 7b, retrosulcus, postauditory, and granular insular cortical areas of *M. fascicularis*. *J Comp Neurol* 192(1): 93-108.
- Roe AW, Ts'o DY. 1995. Visual topography in primate V2: multiple representation across functional stripes. *J Neurosci* 15: 3689-3715.
- Roe AW, Ts'o DY. 1999. Specificity of color connectivity between primate V1 and V2. *J Neurophysiol* 82(5): 2719-2730.
- Roe AW. 2003. Modular complexity of area V2 in the Macaque monkey. *The primate visual system*. Collins C, Kaas J, editors. New York : CRC Press; pp. 109-138.
- Roe AW, Fritsches K, Pettigrew JD. 2005. Optical imaging of functional organization of V1 and V2 in marmoset visual cortex. *Anat Rec A Discov Mol Cell Evol Biol* 287(2): 1213-25.
- Romo R, Hernandez A, Zainos A, Salinas E. 1998. Somatosensory discrimination based on cortical microstimulation. *Nature* 392: 387-390.
- Romo R, Hernandez A, Zainos A, Brody CD, Lemus L. 2000. Sensing without touching: Psychophysical performance based on cortical microstimulation. *Neuron* 26: 273-278.
- Schneider RJ, Friedman DP, Mishkin M. 1993. A modality-specific somatosensory area within the insula of the rhesus monkey. *Brain Res* 621(1): 116-120.
- Schummers J, Marino J, Sur M. 2002. Synaptic integration by V1 neurons depends on location within the orientation map. *Neuron* 36(5): 969-978.
- Schwartz TH, Chen LM, Friedman RM, Spencer DD, Roe AW. 2004. Intraoperative optical imaging of face topography in human somatosensory cortex. *Neuroreport* 15: 1527-1532.
- Sheth BR, Moore CI, Sur M. 1998. Temporal modulation of spatial borders in rat barrel cortex. *J Neurophysiol* 79: 464-470.
- Shoham D, Grinvald A. 2001. The cortical representation of the hand in macaque and human Area S-I: High resolution optical imaging. *J Neurosci* 21: 6820-6835.
- Siegel RM, Raffi M, Phinney RE, Turner JA, Jando G. 2003. Functional architecture of eye position gain fields in visual association cortex of behaving monkey. *J Neurophysiol* 90(2): 1279-1294.
- Spitzer MW, Calford MB, Clarey JC, Pettigrew JD, Roe AW. 2001. Spontaneous and stimulus-evoked intrinsic optical

- signals in primary auditory cortex of the cat. *J Neurophysiol* 85: 1283-1298.
- Sretavan D, Dykes RW. 1983. The organization of two cutaneous submodalities in the forearm region of area 3b of cat somatosensory cortex. *J Comp Neurol* 213: 381-398.
- Sur M. 1980. Receptive fields of neurons in Areas 3b and 1 of somatosensory cortex in monkeys. *Brain Res* 198: 465-471.
- Sur M, Merzenich MM, Kaas JH. 1980. Magnification, receptive-field area, and "hypercolumn" size in areas 3b and 1 of somatosensory cortex in owl monkeys. *J Neurophysiol* 44: 295-311.
- Sur M, Nelson RJ, Kaas JH. 1982. Representations of the body surface in cortical areas 3b and 1 of squirrel monkeys: comparisons with other primates. *J Comp Neurol* 211: 177-192.
- Sur M, Garraghty PE, Bruce C. 1985. Somatosensory cortex in macaque monkeys: laminar differences in receptive field size in areas 3b and 1. *Brain Res* 342: 391-395.
- Sur M, Wall JT, Kaas JH. 1981. Modular segregation of functional cell classes within the postcentral somatosensory cortex of monkeys. *Science* 212: 1059-1061.
- Sur M, Wall JT, Kaas JH. 1984. Modular distribution of neurons with slowly adapting and rapidly adapting responses in area 3b of somatosensory cortex in monkeys. *J Neurophysiol* 51: 724-744.
- Swindale NV. 2000. How many maps are there in visual cortex? *Cereb Cortex* 10: 633-643.
- Talbot WH, Darian-Smith I, Kornhuber HH, Mountcastle VB. 1968. The sense of flutter-vibration: comparison of the human capacity with response patterns of mechanoreceptive afferents from the monkey hand. *J Neurophysiol* 31: 301-334.
- Tanji J, Wise SP. 1981. Submodality distribution in sensorimotor cortex of the unanesthetized monkey. *J Neurophysiol* 45: 467-481.
- Tommerdahl M, Delemos KA, Vierck CJ, Favorov OV, Whitsel BL. 1996. Anterior parietal cortical response to tactile and skin-heating stimuli applied to the same skin site. *J Neurophysiol* 75: 2662-2670.
- Tommerdahl M, Delemos KA, Favorov OV, Metz CB, Vierck CJ, et al. 1998. Response of anterior parietal cortex to different modes of same-site skin stimulation. *J Neurophysiol* 80: 3272-3283.
- Tommerdahl M, Delemos KA, Whitsel BL, Favorov OV, Metz CB. 1999. Response of anterior parietal cortex to cutaneous flutter versus vibration. *J Neurophysiol* 82: 16-33.
- Tommerdahl M, Favorov O, Whitsel BL. 2002. Optical imaging of intrinsic signals in somatosensory cortex. *Behav Brain Res* 135: 83-91.
- Torebjork HE, Ochoa JL. 1980. Specific sensations evoked by activity in single identified sensory units in man. *Acta Physiol Scand* 110: 445-447.
- Ts'o DY, Frostig RD, Lieke EE, Grinvald A. 1990. Functional organization of primate visual cortex revealed by high resolution optical imaging. *Science* 249: 417-420.
- Tsunoda K, Yamane Y, Nishizaki M, Tanifuji M. 2001. Complex objects are represented in macaque inferotemporal cortex by the combination of feature columns. *Nat Neurosci* 4(8): 832-838.
- Vallbo AB. 1981. Sensations evoked from the glabrous skin of the human hand by electrical stimulation of unitary mechanosensitive afferents. *Brain Res* 215(1-2): 359-363.
- Vallbo AB, Johansson RS. 1984. Properties of cutaneous mechanoreceptors in the human hand related to touch sensation. *Hum Neurobiol* 3(1): 3-14.
- Verrillo RT. 1966. Vibrotactile thresholds for hairy skin. *J Exp Psychol* 72(1): 47-50.
- Warren S, Hamalainen HA, Gardner EP. 1986. Objective classification of motion- and direction-sensitive neurons in primary somatosensory cortex of awake monkeys. *J Neurophysiol* 56(3): 598-622.
- Woolsey CN, Marshall WH, Bard P. 1942. Representation of cutaneous tactile sensibility in the cerebral cortex of the monkey as indicated by evoked potentials. *Bull Johns Hopkins Hosp* 70: 399-441.
- Xu X, Bosking W, Sary G, Stefansic J, Shima D, et al. 2004. Functional organization of visual cortex in the owl monkey. *J Neurosci* 24(28): 6237-6247.